Hindawi Publishing Corporation
Advances in Condensed Matter Physics
Volume 2014, Article ID 761960, 9 pages
http://dx.doi.org/10.1155/2014/761960

Research Article

Influence of Codoping on the Optical Properties of ZnO Thin Films Synthesized on Glass Substrate by Chemical Bath Deposition Method

G. Shanmuganathan and I. B. Shameem Banu

Department of Physics, B.S.Abdur Rahman University, Chennai 600048, India

Correspondence should be addressed to G. Shanmuganathan; shan25@bsauniv.ac.in

Received 18 June 2014; Accepted 5 August 2014; Published 31 August 2014

Academic Editor: Weida Hu

Fe and K simultaneously doped ZnO thin films $Zn_{0.99}$ $K_{0.01}$ $(Fe)_x$ O (x = 1, 2, 3, and 4%) were synthesized by chemical bath deposition method. The XRD investigation reveals that all the doped ZnO thin films are in hexagonal wurtzite crystal structure without impurity phases. With increase in Fe concentration, the growth of thin films along c axis is evident from the XRD which indicates the increase in intensity along (002) direction. The same is visible from the surface morphology which shows the formation of hexagonal structure for higher Fe concentration. The topography shows gradual variation with Fe incorporation. The optical energy band gap obtained from the transmittance spectrum decreases from 3.42 to 3.06 eV with increase in Fe concentration indicating the red shift and this trend is consistent with the earlier experimental results. The UV emission is centered around 3.59 eV. The optical constants such as refractive index, extinction coefficient, and absorption coefficient which are essential for the optoelectronic applications were also determined.

1. Introduction

Zinc oxide is an amazing material for numerous applications such as photodetectors, antireflecting coating, thin film solar cell, LEDs, and lithium-ion batteries [1–5] due to its wide band gap (3.445 eV) and high binding energy (60 eV) [1, 6]. Due to its unique optical, semiconductor, and optical properties, ZnO thin films have been extensively studied for various applications. Several methods such as chemical bath deposition, MOCVD, melt growth, ion implementation, DC reactive magnetron cosputtering, and hydrothermal and simple chemical pyrolysis have been used to synthesize ZnO thin films [7–13]. Of late, ZnO thin films are being fabricated by codoping for enhancing the efficiency of ZnO film in optoelectronic devices.

Alkali elements are well-known materials for tuning ZnO optical and electrical behaviors. Alkali doped ZnO films have been broadly investigated in recent decades. Kim et al. reported that, when K doped ZnO thin films were synthesized on Al_2O_3 (001), the optical properties were improved [14]. Xu et al. also reported that the optical emission was emerged while K doped ZnO was annealed during different temperatures [15]. Depending on the different types of substrates such as Si (111), ZnO exhibited different emissions such as green and yellow emissions at 529–567 nm and 600–640 nm due to oxygen vacancy and oxygen interstitials, respectively [16]. For Na-doped ZnO, the carrier mobility was 2.1 cm^2 $V^{-1}S^{-1}$ and structural and optical properties were reported elsewhere [17, 18]. Li doped ZnO is also used for developing the ferroelectric, optical, and multiphonon properties of ZnO semiconductor [19, 20]. In latest decades, Fe doped ZnO has been synthesized for optical properties [21] because Fe is well-known optical emitter in doped ZnO. Zhang et al. reported [22] that the optical mechanism of ZnO alloyed with Fe ion. Not only optical properties but also Fe is well known as a doping element for altering the magnetic and electrical properties [23–25]. The extensive literature survey shows that only few works were reported on the optical properties of dual doped ZnO films. Some experimental works such as Al-K [26], Li-N [27], Li-Mg [28], Fe-Co [29], and Fe-N [30]

reported the dual doped ZnO to investigate the optical and magnetic properties. However, the combination of alkali and transition metals (TM) dual doped ZnO is rarely reported.

As per the literature till date the study on the optical properties of K and Fe doped ZnO thin films has not been reported yet. Both Fe and K when doped to ZnO separately, they modify the band gap and also the luminescence characteristics and hence, the Fe and K simultaneously doped to ZnO can bring out some interesting results and so in the present study, (K, Fe) codoped ZnO thin films were investigated for the influence on the optical properties. The optical properties of K doped ZnO films show that 1% of K exhibited better optical properties [31]. For further optical investigation, the transition metal Fe is added into ZnO:K (1%) due to its excellent optical emission property. The simple chemical bath deposition method is employed to fabricate these films. The influence of Fe concentration on the optical behavior has been revealed in the transmittance and photoluminescence sections. In the present work, 1% K doped ZnO would be indicated as ZnO:K (1%). The main purpose of this study is to examine the effect of Fe ion concentration on optical properties of ZnO:K (1%) films.

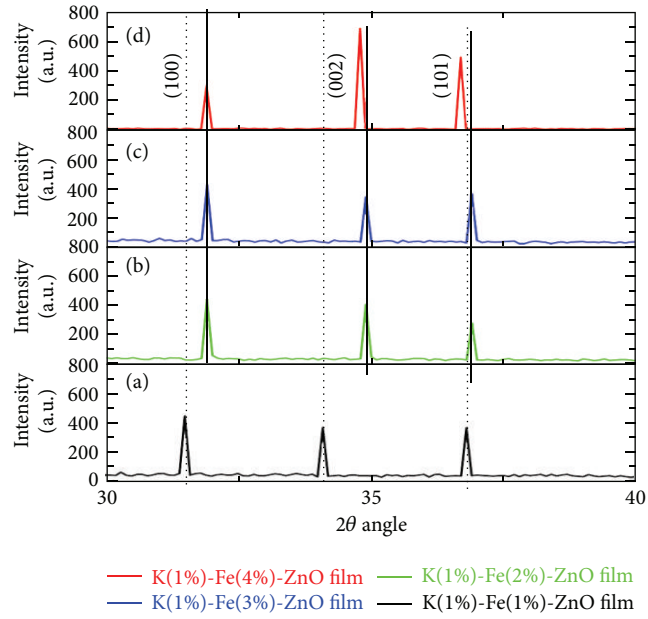

Figure 1: XRD pattern of (K (1%), Fe) codoped ZnO for Fe concentrations: (a) 1%, (b) 2%, (c) 3%, and (d) 4%.

2. Experimental Work

Codoped (K, Fe) ZnO films were synthesized by chemical bath deposition method. Here, $ZnCl_2$ (AR MERCK), KOH (AR MERCK), KCH_3COO (AR MERCK), and $FeSO_4 \cdot 7H_2O$ (AR MERCK) were the precursor materials and doping source materials, respectively. Initially, $ZnCl_2$ and KOH were dissolved in the triple distilled water with 1 : 1 ratio and stirred using magnetic stirrer at 60°C for 10 minutes. Then one percentage of potassium acetate was added in 1 : 1 ratio prepared homogeneous solution. After that, different percentages of Fe (1 at %, 2 at %, 3 at %, and 4 at %) were added to the solution for doping. In the synthesized homogenous solution, HCl is added to keep the pH at 8. The solution was cooled to room temperature and microglass slide was used as substrate. The substrate was cleaned by HCl, acetone, and double distilled water. Then the cleaned substrate was immersed vertically in the solution using substrate holder. Finally, the solution was steadily stirred by magnetic stirrer to get the uniformly coating on the substrate. After 45 minutes of deposition, the uniform coated substrates were taken out from the solutions and cleaned with double distilled water and then dried in air. Finally, thin films are kept in the furnace and calcined at 400°C for 1 hour.

3. Results and Discussion

3.1. Structural Analysis. The XRD pattern of codoped (K, Fe) ZnO thin films is shown in Figure 1. All the thin films exhibit hexagonal crystal phase and it is confirmed with standard JCPDS card (PDF numbers 891397 and 890510) number. In XRD pattern, the three prominent peaks such as (100), (002), and (101) were obtained for all films without any secondary phase. In our previous report, three prominent peaks such as (100), (002), and (101) were observed for ZnO:K (1%) thin film [31]. In the present work, when Fe concentration is increased, the crystal properties of the codoped ZnO thin films have changed. The low intensity peak was observed for ZnO:K (1%) [31]. However, in the present work, it is observed that when Fe is introduced, the intensity of three prominent peaks has changed. The variation in intensity indicates the incorporation of Fe ions in the lattice of ZnO site. In the doping process, the three prominent peaks are shifted from higher to lower angles due to the different ionic radius of Fe such as Fe^{3+} and Fe^{2+}. For 2, 3, and 4% of Fe, the three prominent peaks shifted to higher angle than 1% Fe due to the inclusion of Fe^{3+} (0.068 nm) [11, 32]. For 4% Fe, the (002) peak shifts to lower angle due to the high ionic radius (0.078) of Fe^{2+} [33, 34]. In the entire XRD pattern, the intensity of (002) plane varied for different Fe ion concentrations which indicates that the film is grown along *c*-axis. In the XRD pattern, the high intensity of (002) plane reveals the improved crystallinity [35]. The full width at half maximum of (002) peaks is significantly varied with various Fe concentrations. For 4% Fe, the FWHM is lower than others. Saha et al. reported that the low FWHM reveals the deterioration of the crystallinity [36]. For the codoped ZnO film, average crystal size and average crystal strain were calculated and are summarized in Table 1.

The crystalline sizes of thin films are calculated using Scherrer formula:

$$D = \frac{0.9\lambda}{\beta \cos\theta} \quad (1)$$

3.2. Surface Morphology Analysis and EDAX Spectrum. Figure 2 shows the surface morphology of (K, Fe) codoped ZnO films investigated by field emission scanning electron

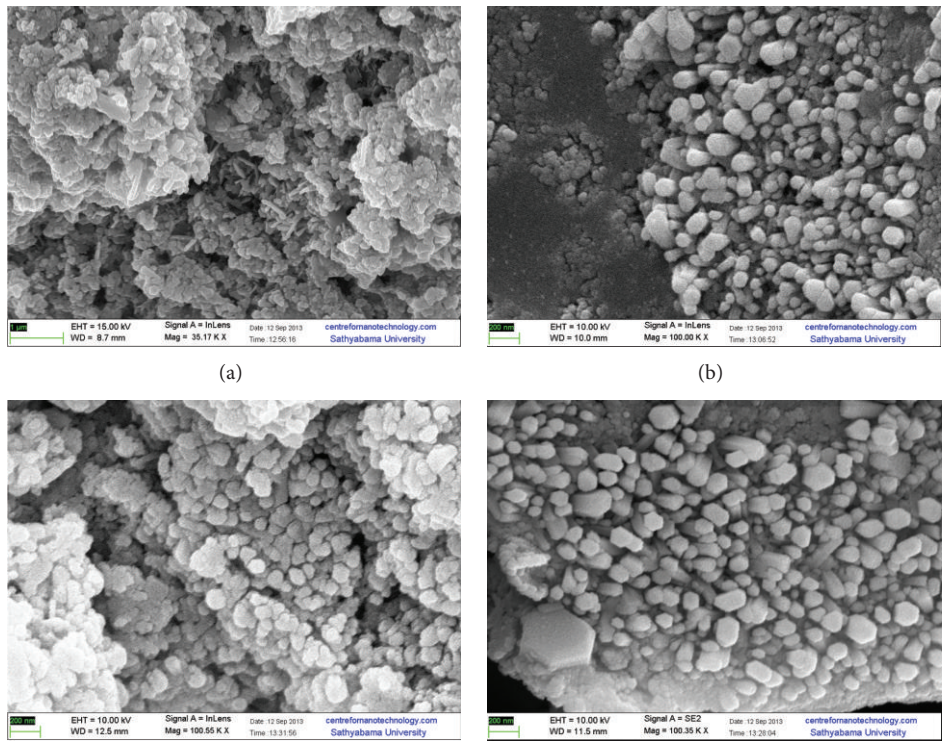

FIGURE 2: Surface morphology (FESEM) of (K (1%), Fe) codoped ZnO for Fe concentrations: (a) 1%, (b) 2%, (c) 3%, and (d) 4%.

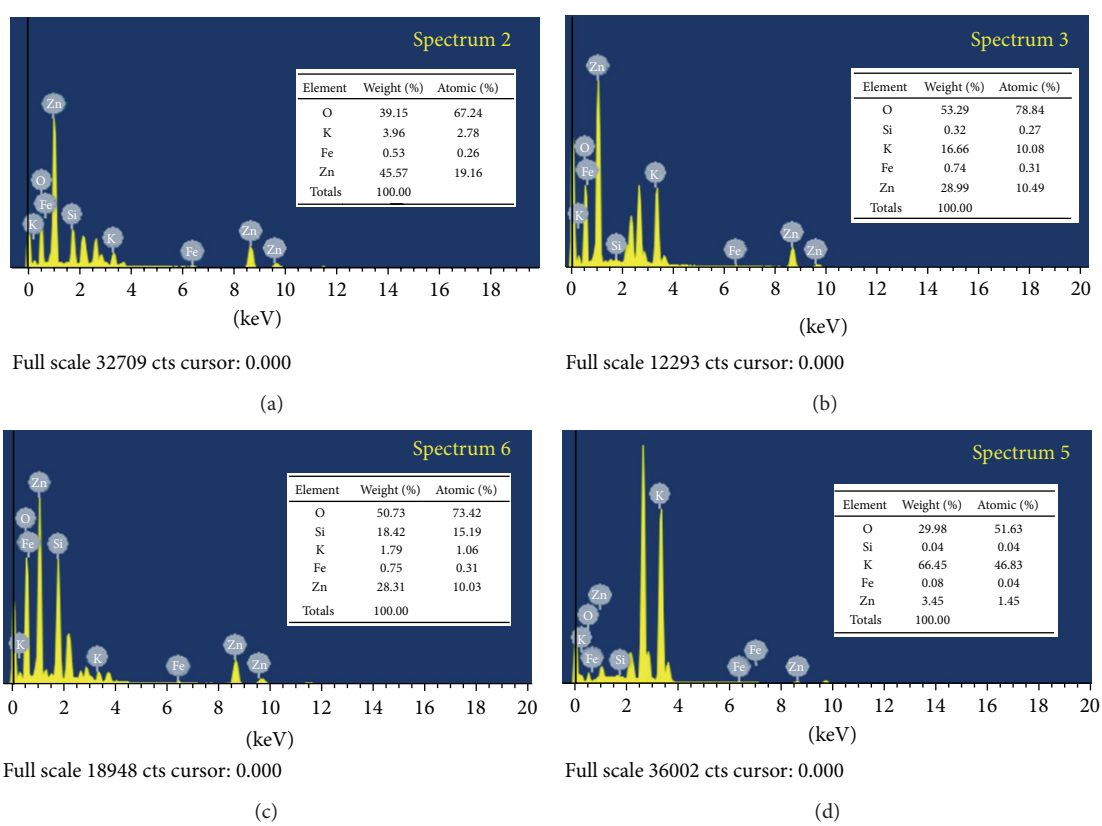

FIGURE 3: EDAX spectrum of (K (1%), Fe) codoped ZnO for Fe concentrations: (a) 1%, (b) 2%, (c) 3%, and (d) 4%.

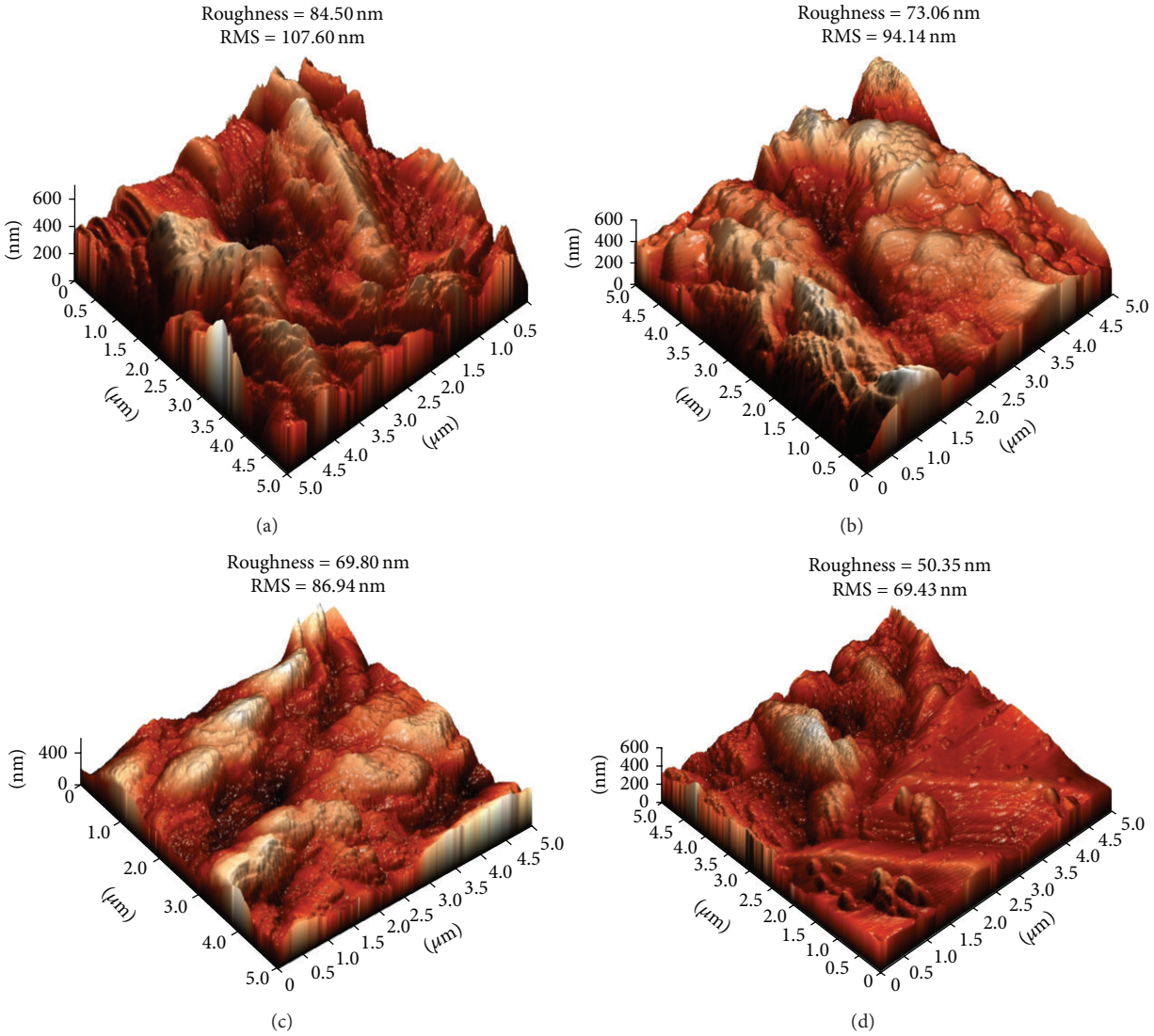

Figure 4: Atomic force microscope of (K (1%), Fe) codoped ZnO for Fe concentrations: (a) 1%, (b) 2%, (c) 3%, and (d) 4%.

microscope (SUPRA "55"). SEM image shows that morphology changes with Fe doping concentrations. The film exhibits small grains of varied size at different level of Fe. The element compositions such as Zn, O, K, and Fe were confirmed by energy dispersive analysis X-ray spectroscopy and are shown in Figure 3. In all EDAX spectrums, the substrate peak is presented between 2.4 and 2.5 eV [31].

3.3. Surface Topology. In Figure 4 three-dimensional (3D) surface topography of (K, Fe) codoped ZnO thin films is presented. Surface topography was scanned at $5 \times 5\,\mu$m in tapping mode. The average roughness and root mean square values were determined. The average roughness is 84.50 nm, 73.06 nm, 69.80 nm, and 50.35 nm at level 1, 2, 3, and 4% Fe, respectively. The RMS values are 107.60 nm, 94.14 nm, 86.94 nm, and 69.43 nm for 1, 2, 3, and 4 at % Fe, respectively. The decreases in average roughness and RMS show that the crystalline quality of the codoped ZnO thin films has been improved by increase in Fe concentration. The low roughness indicates the enhancement of crystalline quality [37].

3.4. Transmittance Spectrum and Optical Band Gap. The transmittance spectrum of (K, Fe) codoped ZnO nanofilms is shown in Figure 5. The (K, Fe) codoped ZnO thin films exhibit a low transmittance as seen in Figure 5. In the visible region, the transmittance is 50%, 45%, 25%, and 10% for 1, 2, 3, and 4 at % Fe, respectively, and the transmittance is found to decrease with increase in Fe dopant concentration. The film thickness is one of the main factors for low transmittance. In the doping process, the film thickness is 4.348 μm, 4.690 μm, 5.078 μm, and 6.520 μm for 1, 2, 3, and 4% Fe, respectively. Xu et al. have reported that the optical transmittance obviously reduced in the visible region due to the Fe ion concentrations [38, 39]. Prajapati et al. have studied that the low transmittance was obtained for Fe doped ZnO thin films due to lattice defects into ZnO lattice [40].

Table 1: The peak position, FWHM, average crystalline size, lattice constant, and average lattice strain for the (K, Fe) codoped ZnO thin films.

Materials	Peak positions			FWHM of peaks			Average crystalline size (nm)	Lattice constant (nm)		Average crystalline strain (nm)
	(100)	(002)	(001)	(100)	(002)	(101)		a	b	
K (1%)-Fe (1%)-ZnO film	31.49	34.10	36.80	0.1088	0.1060	0.1076	77.39	0.3043	0.5270	0.0879
K (1%)-Fe (2%)-ZnO film	31.90	34.90	36.90	0.1105	0.1095	0.1081	76.47	0.2862	0.4957	0.0882
K (1%)-Fe (3%)-ZnO film	31.90	34.90	36.90	0.1102	0.1093	0.1088	76.08	0.3004	0.5203	0.0882
K (1%)-Fe (4%)-ZnO film	31.90	34.80	36.70	0.1014	0.1009	0.1002	82.55	0.3012	0.5217	0.0815

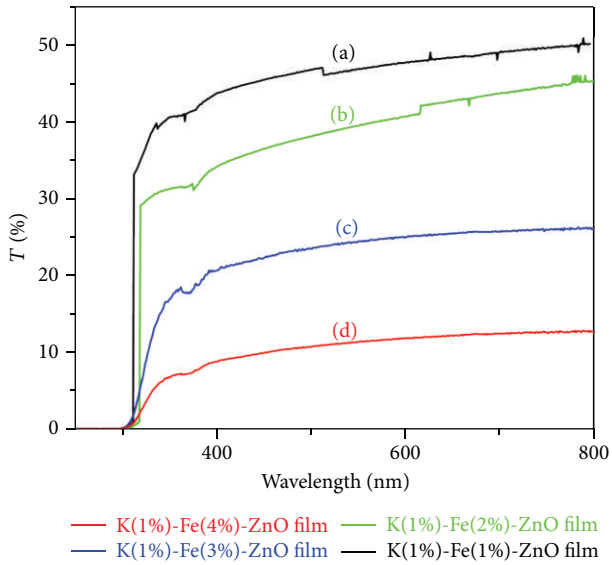

Figure 5: UV transmittance of (K (1%), Fe) codoped ZnO for Fe concentrations: (a) 1%, (b) 2%, (c) 3%, and (d) 4%.

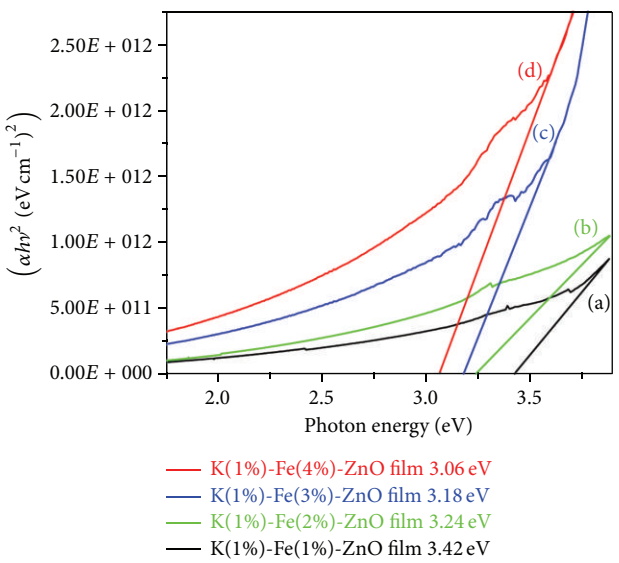

Figure 6: Optical band gap of (K (1%), Fe) codoped ZnO for Fe concentrations: (a) 1%, (b) 2%, (c) 3%, and (d) 4%.

Due to the film thickness, the incident light is much absorbed and so the transmittance light intensity is less pronounced. This fact is well reported by the absorption coefficient values of these thin films (Figure 9).

The optical band gap of codoped (K, Fe) nano-ZnO films is calculated from the following formula:

$$\alpha = \frac{1}{d}\ln\left(\frac{1}{T}\right),$$
$$(\alpha h\nu)^2 = A\left(h\nu - E_g\right), \tag{2}$$

where $h\nu$ is photon energy and E_g is energy gap. The optical band gaps of codoped ZnO films are shown in Figure 6. The optical energy gap can be obtained by extrapolating the linear part to x-axis. In our previous work, the band gap was 3.94 eV for ZnO:K (1%) film [31]. The energy gap reduces due to the increase in Fe doping concentration. The band gap values are 3.42 eV, 3.24 eV, 3.18 eV, and 3.06 eV for 1, 2, 3, and 4 at % Fe, respectively, thus indicating the red shift. C. S. Prajapati et al. reported that when Fe ion was doped with ZnO, the optical band gap changes [40]. However, Xu and Li reported that the band gap of ZnO was increased by Fe ion concentrations [38]. The red shift was also observed for ZnO thin films due to the high doping material, renormalization effect [41], and film thickness [21, 42]. Among the three factors, the change in the optical band gap also depends on the thickness of the thin film.

3.5. Optical Constants. The refractive index of codoped ZnO films is calculated from the following formula:

$$n = \left(\frac{1+R}{1-R}\right) + \sqrt{\left(\frac{4R}{(1-R)^2}\right) - k^2},$$
$$k = \frac{\alpha\lambda}{4\pi}. \tag{3}$$

The refractive index of codoped ZnO thin films as function of wavelength is shown in Figure 7. The refractive index varies with variation in Fe concentrations. In the visible region the light is normally dispersed due to the contribution of virtual electronic transition [43] and lower dense medium. For the 375 nm, the refractive index of codoped ZnO thin film is 5.3, 3.2, 4.3, and 6.2 for 1, 2, 3, and 4% Fe, respectively. The thin

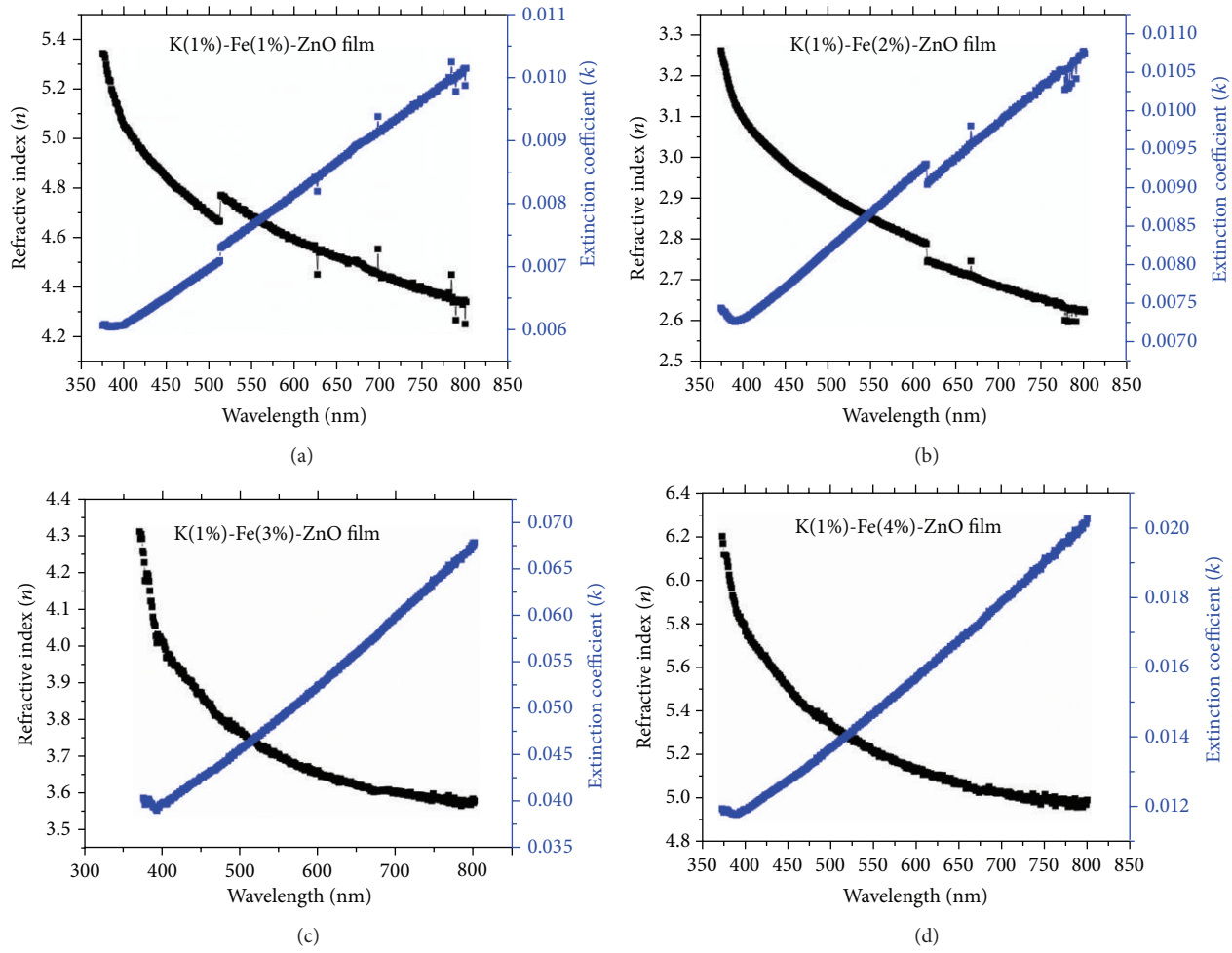

Figure 7: Refractive index of (K (1%), Fe) codoped ZnO for Fe concentrations: (a) 1%, (b) 2%, (c) 3%, and (d) 4%.

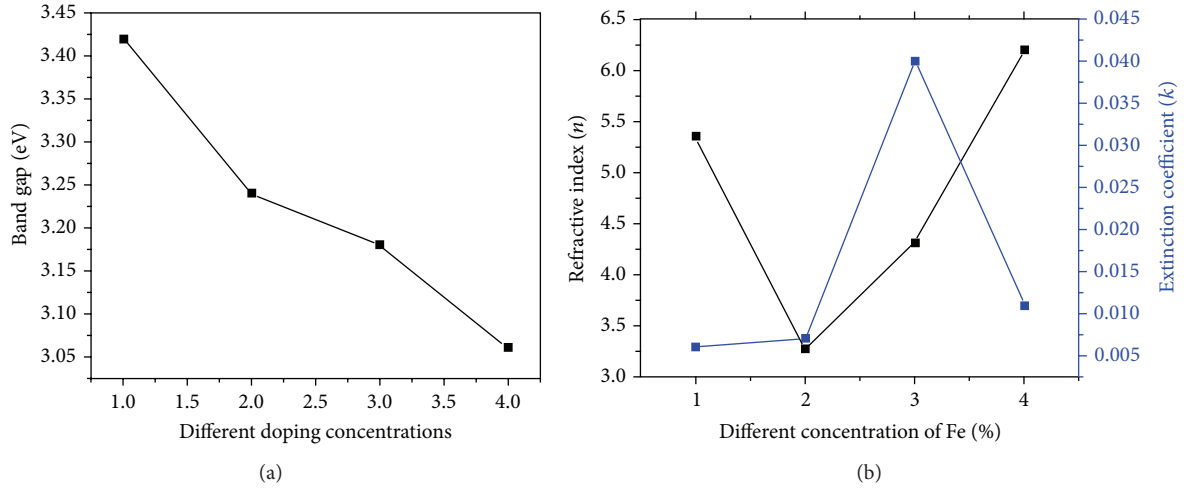

Figure 8: The figure shows (a) band gap versus different Fe % and (b) refractive index and extinction coefficient versus different Fe %.

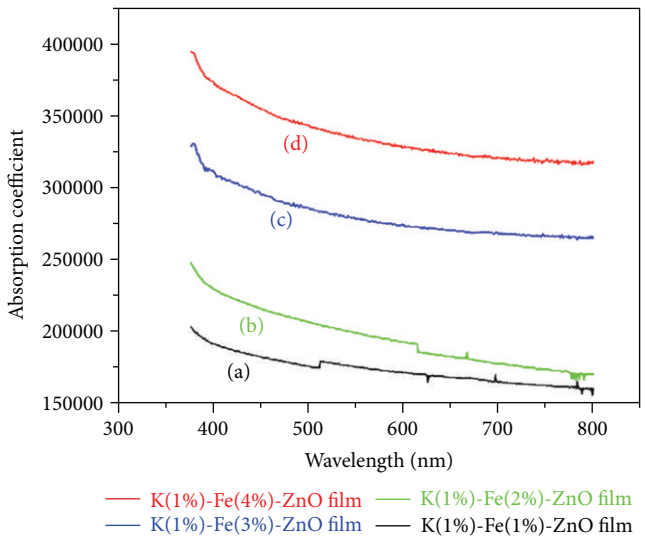

FIGURE 9: Absorption coefficient of (K (1%), Fe) codoped ZnO for Fe concentrations: (a) 1%, (b) 2%, (c) 3%, and (d) 4%.

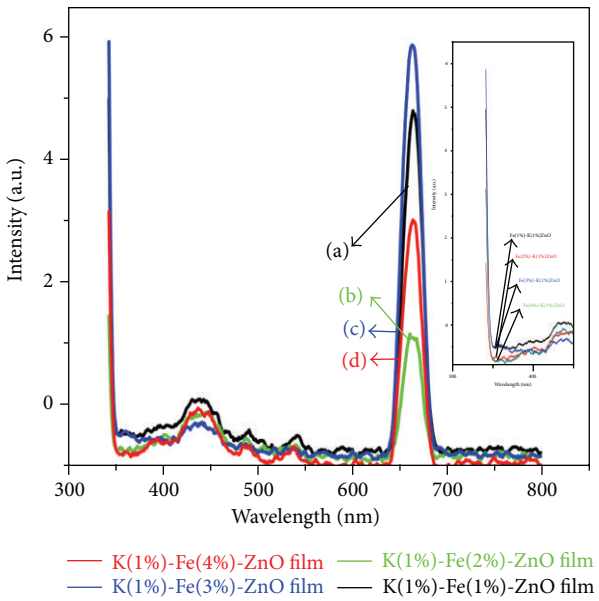

FIGURE 10: Photoluminescence spectrum of (K (1%), Fe) codoped ZnO for Fe concentrations: (a) 1%, (b) 2%, (c) 3%, and (d) 4%.

films exhibit significant changes and are also suitable for integrated optical device application. The normal dispersion indicates that the films do not have voids or any defects. The lower values of extinction coefficient indicate the smoothness of the thin film.

Figure 8 shows the variation of optical band gap, refractive index, and extinction coefficient of Fe concentrations. In Figure 8(a), the optical band gap decreases significantly with increases in Fe concentrations. Figure 8(b) shows that the refractive index of codoped ZnO films is increased (at $\lambda = 375$ nm) considerably for different doping (Fe) concentrations. This indicates that the light normally travels through the medium. Moreover, the extinction coefficient (k) reveals the well smoothness of thin films surface.

Figure 9 shows the absorption coefficient (α) of (K, Fe) codoped ZnO thin films for different Fe doping concentrations. For ZnO:K (1%), α was $2.75 \times 10^5\,\text{cm}^{-1}$ [31]. In the UV region at $\lambda = 375$ nm, absorption coefficient is $2.03 \times 10^5\,\text{cm}^{-1}$, $2.48 \times 10^5\,\text{cm}^{-1}$, $3.30 \times 10^5\,\text{cm}^{-1}$, and $3.95 \times 10^5\,\text{cm}^{-1}$ for 1, 2, 3, and 4% of Fe, respectively. In the present investigation, in the UV region, the absorption of light depends on the thickness of the film. The higher absorption of ZnO thin films is suitable for antireflecting coating (ARC) and optoelectronic applications [44].

3.6. Photoluminescence Study. Figure 10 shows the photoluminescence spectrum of (K, Fe) codoped ZnO films at room temperature. Generally, UV emissions exist in the range between 360 nm and 380 nm [45]. The UV emission was observed at 389 nm for ZnO:K (1%) [31]. In the present PL spectrum, UV emission appears around 345 nm (3.59 eV) due to the free exciton [46]. However, in the photoluminescence spectrum, the intensity of UV emission significantly varies for 1, 2, and 3% of Fe ion concentrations but the UV intensity is reduced for 4% Fe ion concentration. This may be due to the low concentration of Zn and O and it can be seen in EDAX spectrum. This is the evidence for the variation of UV intensity in the photoluminescence. The weak blue emission is presented with low intensity at 437 nm due to the low interstitial of Zn [47]. The red emission is obtained in the range between 661 nm and 663 nm due to the surplus of oxygen or interstitials of oxygen [48]. The peak position of the photoluminescence depends on the contribution between the free exciton and transition between free electrons to acceptor bound holes [49]. And also the position and intensity of UV and red emissions in PL are enhanced by incorporation of Fe ion in ZnO lattice site. In this study photoluminescence spectrum clearly reveals that the codoped ZnO thin films are defect free.

4. Conclusion

In the current work, the optical properties of (K, Fe) codoped ZnO thin films synthesized on glass substrate by chemical bath deposition technique have been investigated. The X-ray diffraction analysis confirms the hexagonal crystal structure of ZnO thin films. The grains with hexagonal morphology were observed for different Fe ion concentrations. The average thin film surface roughness decreases with increase of Fe ion concentration. The optical transmittance decreases due to the film thickness. The optical band gap of codoped ZnO thin films decreases due to different doping concentration. The different optical properties such as refractive index and absorption coefficient revealed that the optical behavior of thin films and the low extinction coefficient value indicate the better quality of the film. The absorption coefficient shows an increase with doping concentration. The photoluminescence spectrum revealed that the codoped ZnO thin films are mostly defect free. The present study shows that codoped (K,

Fe) ZnO thin films can be suitable candidates for antireflecting coating (ARC) and optoelectronic devices.

Conflict of Interests

The authors declare that there is no conflict of interests regarding the publication of this paper.

References

[1] S. M. Hatch, J. Briscoe, A. Sapelkin et al., "Influence of anneal atmosphere on ZnO-nanorod photoluminescent and morphological properties with self-powered photodetector performance," *Journal of Applied Physics*, vol. 113, no. 20, Article ID 204501, 2013.

[2] Y. Lu, X. Zhang, J. Huang et al., "Investigation on antireflection coatings for Al:ZnO in silicon thin-film solar cells," *Optik*, vol. 124, no. 18, pp. 3392–3395, 2013.

[3] M. Bär, J.-P. Theisen, R. G. Wilks et al., "Lateral inhomogeneity of the Mg/(Zn+Mg) composition at the (Zn,Mg)O/CuIn(S,Se)2 thin-film solar cell interface revealed by photoemission electron microscopy," *Journal of Applied Physics*, vol. 113, no. 19, Article ID 193709, 2013.

[4] R. Juday, E. M. Silva, J. Y. Huang, P. G. Caldas, R. Prioli, and F. A. Ponce, "Strain-related optical properties of ZnO crystals due to nanoindentation on various surface orientations," *Journal of Applied Physics*, vol. 113, no. 18, Article ID 183511, 2013.

[5] S. M. Abbas, S. T. Hussain, S. Ali, N. Ahmad, N. Ali, and S. Abbas, "Structure and electrochemical performance of ZnO/CNT composite as anode material for lithium-ion batteries," *Journal of Materials Science*, vol. 48, no. 16, pp. 5429–5436, 2013.

[6] Z. Zeng, C. S. Garoufalis, A. F. Terzis, and S. Baskoutas, "Linear and nonlinear optical properties of ZnO/ZnS and ZnS/ZnO core shell quantum dots: effects of shell thickness, impurity, and dielectric environment," *Journal of Applied Physics*, vol. 114, no. 2, Article ID 023510, 2013.

[7] D. Chu, T. Hamada, K. Kato, and Y. Masuda, "Growth and electrical properties of ZnO films prepared by chemical bath deposition method," *Physica Status Solidi A*, vol. 206, no. 4, pp. 718–723, 2009.

[8] D. N. Montenegro, V. Hortelano, O. Martínez et al., "Influence of metal organic chemical vapour deposition growth conditions on vibrational and luminescent properties of ZnO nanorods," *Journal of Applied Physics*, vol. 113, no. 14, Article ID 143513, 2013.

[9] W. Mtangi, M. Schmidt, F. D. Auret et al., "A study of the T_2 defect and the emission properties of the E3 deep level in annealed melt grown ZnO single crystals," *Journal of Applied Physics*, vol. 113, no. 12, Article ID 124502, 2013.

[10] J. E. Stehr, X. J. Wang, S. Filippov et al., "Defects in N, O and N, Zn implanted ZnO bulk crystals," *Journal of Applied Physics*, vol. 113, no. 10, Article ID 103509, 2013.

[11] G. Chen, J. J. Peng, C. Song, F. Zeng, and F. Pan, "Interplay between chemical state, electric properties, and ferromagnetism in Fe-doped ZnO films," *Journal of Applied Physics*, vol. 113, no. 10, Article ID 104503, 2013.

[12] J. Joo, B. Y. Chow, M. Prakash, E. S. Boyden, and J. M. Jacobson, "Face-selective electrostatic control of hydrothermal zinc oxide nanowire sythesis," *Nature Materials*, vol. 10, pp. 596–601, 2011.

[13] S. S. Shinde, A. P. Korade, C. H. Bhosale, and K. Y. Rajpure, "Influence of tin doping onto structural, morphological, optoelectronic and impedance properties of sprayed ZnO thin films," *Journal of Alloys and Compounds*, vol. 551, pp. 688–693, 2013.

[14] S.-K. Kim, S. A. Kim, C.-H. Lee, H.-J. Lee, S.-Y. Jeong, and C. R. Cho, "The structural and optical behaviors of K-doped $ZnO/Al_2O_3(0001)$ films," *Applied Physics Letters*, vol. 85, no. 3, pp. 419–421, 2004.

[15] L. Xu, F. Gu, J. Su, Y. Chen, X. Li, and X. Wang, "The evolution behavior of structures and photoluminescence of K-doped ZnO thin films under different annealing temperatures," *Journal of Alloys and Compounds*, vol. 509, no. 6, pp. 2942–2947, 2011.

[16] J. Lü, K. Huang, J. Zhu, X. Chen, X. Song, and Z. Sun, "Preparation and characterization of Na-doped ZnO thin films by sol-gel method," *Physica B*, vol. 405, no. 15, pp. 3167–3171, 2010.

[17] W. Liu, F. Xiu, K. Sun et al., "Na-doped p-type ZnO microwires," *Journal of the American Chemical Society*, vol. 132, no. 8, pp. 2498–2499, 2010.

[18] S. Kumar and R. Thangavel, "Structural and optical properties of Na doped ZnO nanocrystalline thin films synthesized using sol-gel spin coating technique," *Journal of Sol-Gel Science and Technology*, vol. 67, no. 1, pp. 50–55, 2013.

[19] M. Joseph, H. Tabata, and T. Kawai, "Ferroelectric behavior of Li-doped ZnO thin films on Si(100) by pulsed laser deposition," *Applied Physics Letters*, vol. 74, no. 17, pp. 2534–2536, 1999.

[20] S. Kalyanaraman, R. Vettumperumal, and R. Thangavel, "Study of multiple phonon behavior in Li-doped ZnO thin films fabricated using the sol-gel spin-coating technique," *Journal of the Korean Physical Society*, vol. 62, no. 5, pp. 804–808, 2013.

[21] T. Rattana, S. Suwanboon, P. Amornpitoksuk, A. Haidoux, and P. Limsuwan, "Improvement of optical properties of nanocrystalline Fe-doped ZnO powders through precipitation method from citrate-modified zinc nitrate solution," *Journal of Alloys and Compounds*, vol. 480, no. 2, pp. 603–607, 2009.

[22] Y. Zhang, L. Wu, H. Li et al., "Influence of Fe doping on the optical property of ZnO films," *Journal of Alloys and Compounds*, vol. 473, no. 1-2, pp. 319–322, 2009.

[23] M. Benhaliliba, Y. S. Ocak, and A. Tab, "Characterization of coated fe-doped zinc oxide nanostructures," *Journal of Nano- & Electronic Physics*, vol. 5, no. 3, 2013.

[24] J. Wang, J. Wan, and K. Chen, "Facile synthesis of superparamagnetic Fe-doped ZnO nanoparticles in liquid polyols," *Materials Letters*, vol. 64, no. 21, pp. 2373–2375, 2010.

[25] A. Sawalha, M. Abu Abdeen, and A. Sedky, "Electrical conductivity study in pure and doped ZnO ceramic system," *Physica B*, vol. 404, no. 8–11, pp. 1316–1320, 2009.

[26] J. Xu, S. Shi, X. Zhang, and Y. Wang, "Structural and optical properties of (Al, K)-co-doped ZnO thin films deposited by a sol-gel technique," *Materials Science in Semiconductor Processing*, vol. 16, no. 3, pp. 732–737, 2013.

[27] D. Zhang, J. Zhang, Z. Guo, and X. Miao, "Optical and electrical properties of zinc oxide thin films with low resistivity via Li-N dual-acceptor doping," *Journal of Alloys and Compounds*, vol. 509, no. 20, pp. 5962–5968, 2011.

[28] S. Aksoy, Y. Caglar, S. Ilican, and M. Caglar, "Sol-gel derived Li-Mg co-doped ZnO films: preparation and characterization via XRD, XPS, FESEM," *Journal of Alloys and Compounds*, vol. 512, no. 1, pp. 171–178, 2012.

[29] J. J. Beltrán, J. A. Osorio, C. A. Barrero, C. B. Hanna, and A. Punnoose, "Magnetic properties of Fe doped, Co doped, and Fe+Co co-doped ZnO," *Journal of Applied Physics*, vol. 113, no. 17, Article ID 17C308, 2013.

[30] S. Ghosh, M. Mandal, and K. Mandal, "Effects of Fe doping and Fe–N-codoping on magnetic properties of SnO_2 prepared by chemical co-precipitation," *Journal of Magnetism and Magnetic Materials*, vol. 323, no. 8, pp. 1083–1087, 2011.

[31] G. Shanmuganathan, I. B. S. Banu, S. Krishnan, and B. Ranganathan, "Influence of K-doping on the optical properties of ZnO thin films grown by chemical bath deposition method," *Journal of Alloys and Compounds*, vol. 562, pp. 187–193, 2013.

[32] B. Zhang, S. Zhou, H. Wang, and Z. Du, "Raman scattering and photoluminescence of Fe-doped ZnO nanocantilever arrays," *Chinese Science Bulletin*, vol. 53, no. 11, pp. 1639–1643, 2008.

[33] C. S. Prajapati, A. Kushwaha, and P. P. Sahay, "Experimental investigation of spray-deposited Fe-doped ZnO nanoparticle thin films: structural, microstructural and optical properties," *JTTEES*, vol. 22, p. 1232, 2013.

[34] L. Xu and X. Li, "Influence of Fe-doping on the structural and optical properties of ZnO thin films prepared by sol-gel method," *Journal of Crystal Growth*, vol. 312, no. 6, pp. 851–855, 2010.

[35] L. C. Yang, R. X. Wang, S. J. Xu et al., "Effects of annealing temperature on the characteristics of Ga-doped ZnO film metal-semiconductor-metal ultraviolet photodetectors," *Journal of Applied Physics*, vol. 113, no. 8, Article ID 084501, 2013.

[36] S. Saha and V. Gupta, "Al and Fe co-doped transparent conducting ZnO thin film for mediator-less biosensing application," *Journal of Applied Physics*, vol. 1, Article ID 042112, 3 pages, 2013.

[37] K. A. Eswar, A. Azlinda, H. F. Husairi, M. Rusop, and S. Abdullah, "Post annealing effect on thin film composed ZnO nano-particles on porous silicon," *Nano Bulletin*, vol. 2, p. 130212-3, 2013.

[38] L. Xu and X. Li, "Influence of Fe-doping on the structural and optical properties of ZnO thin films prepared by sol-gel method," *Journal of Crystal Growth*, vol. 312, no. 6, pp. 851–855, 2010.

[39] S. M. Salaken, E. Farzana, and J. Podder, "Effect of Fe-doping on the structural and optical properties of ZnO thin films prepared by spray pyrolysis," *Chinese Institute of Electronics*, vol. 34, Article ID 073003, 6 pages, 2013.

[40] C. S. Prajapati, A. Kushwaha, and P. P. Sahay, "Experimental investigation of spray-deposited fe-doped ZnO nanoparticle thin films: structural, microstructural, and optical properties," *Journal of Thermal Spray Technology*, vol. 22, no. 7, pp. 1230–1241, 2013.

[41] T. Wang, Y. Liu, Q. Fang et al., "Morphology and optical properties of Co doped ZnO textured thin films," *Journal of Alloys and Compounds*, vol. 509, no. 37, pp. 9116–9122, 2011.

[42] M. Öztas and M. Bedir, "Thickness dependence of structural, electrical and optical properties of sprayed ZnO:Cu films," *Thin Solid Films*, vol. 516, no. 8, pp. 1703–1709, 2008.

[43] A. A. Ziabari and F. E. Ghodsi, "Optoelectronic studies of sol-gel derived nanostructured CdO-ZnO composite films," *Journal of Alloys and Compounds*, vol. 509, no. 35, pp. 8748–8755, 2011.

[44] Q. G. Du, G. Alagappan, H. Dai et al., "UV-blocking ZnO nanostructure anti-reflective coatings," *Optics Communications*, vol. 285, no. 13-14, pp. 3238–3241, 2012.

[45] O. Lupana, T. Pauporte, L. Chowc et al., "Effects of annealing on properties of ZnO thin films prepared by electrochemical deposition in chloride medium," *Applied Surface Science*, vol. 256, pp. 1895–1907, 2010.

[46] Z. R. Khan, M. S. Khan, M. Zulfequar, and M. S. Khan, "Optical and structural properties of ZnO thin films fabricated by Sol-Gel method," *Materials Sciences and Applications*, vol. 2, no. 5, pp. 340–345, 2011.

[47] B. Y. Erdoan, "The alloying effects on the structural and optical properties of nanocrystalline copper zinc oxide thin films fabricated by spin coating and annealing method," *Journal of Alloys and Compounds*, vol. 502, no. 2, pp. 445–450, 2010.

[48] A. S. Kuznetsov, Y.-G. Lu, S. Turner et al., "Preparation, structural and optical characterization of nanocrystalline ZnO doped with luminescent Ag-nanoclusters," *Optical Materials Express*, vol. 2, no. 6, pp. 723–734, 2012.

[49] M. Gao, J. Yang, L. Yang et al., "Enhancement of optical properties and donor-related emissions in Y-doped ZnO," *Superlattices and Microstructures*, vol. 52, no. 1, pp. 84–91, 2012.